

NUMERICAL ANALYSIS OF THIN WALLED BEAMS WITH INTERNAL UNBONDED CABLES BY THE RITZ METHOD

A. DALL'ASTA and G. LEONI

Department of Structural Engineering, University of Ancona, Ancona, Italy

(Received 23 April 1996, in revised form 20 January 1997)

Abstract—The authors analyze the behavior of thin walled beams crossed by internal stretched cables anchored at their ends but free to slip without friction along their path, by using a previously presented model. The guidelines for the numerical solution of the linear elastic problem and the stability analysis are presented in general form and applied to a class of problems of technical interest. The numerical analysis examines the case of simply supported beam with symmetric open cross section, crossed by a cable placed on rectilinear or parabolic paths lying in the symmetry plane, assuming as problem variables the beam stiffness, the parameters describing the cable path and the cable traction force. This permitted evidencing some aspects of the problem of interest in structural engineering, by showing the relations between stress increments of beam and cable under external force and the complex relations arising between beam bending, torsional and shear stiffness, cable path, cable traction force and external load in the stability analysis. © 1997 Elsevier Science Ltd.

NOTATION

A = matrix of the coefficient in the elastic analysis
B^r = matrix of the geometrical effects due to the cable prestressing
B^e = matrix of the geometrical effects due to the external actions
H = depth of the cross section
l = vector of known terms in the elastic analysis
s = eccentricity of the cable anchorage at the end cross section of the beam
w = vector of the shape function coefficients
W = matrix of the stress geometrical effects (eqns (62) and (66))
*x*_{*i*} = co-ordinate of the cross section point
*y*_{*i*} = shape function
Y = shape function matrix

For symbols not reported, reader can refer to Dall'Asta and Leoni (1997)

1. INTRODUCTION

In the previous paper "Thin walled beams with internal unbonded cables: balance conditions and stability" (Dall'Asta and Leoni (1997)) the authors presented a model for the analysis of beams containing a stretched cable draped along an internal protective tube, furnishing a synthetic outline of the technical importance of such a coupled system and a review of the existing literature on the topic. The cited work was mainly dedicated to the balance conditions of the problem by referring to a kinematical model able to describe the effects due to shear strains related to torsion and shear in thin walled cross sections. Two linear formulations describing the behavior in the neighborhood of the natural state and in the neighborhood of a balanced stressed state were obtained, the former in order to determine the stress and strain provided by the controllable cable force and external actions and the latter in order to investigate the infinitesimal stability of balanced configurations. Some characteristic aspects of the problem were evidenced under a qualitative point of view only.

In this paper the numerical solution of the problem formulation previously presented is approached with the variational method, by approximating axis displacements, cross section rotations and warping functions through shape functions satisfying natural boundary conditions. Both the problem of evaluating the stress and strain induced by external loads and the problem of determining the critical conditions for stability are dealt with and some considerations on numerical procedures are reported.

Applications contained in this work analyze some real cases of technical interest in order to evaluate the effectiveness of such a coupled system. In particular, the results reported refer to a symmetric thin walled beam undergoing transverse loads and evaluate the consequences, in terms of stiffness and stability behavior, deriving from different geometries of the cable path and different values of the cable force. The beam geometries, the constitutive parameters and the range of actions considered allow the results to be applied to concrete and steel beams crossed by high strength steel cables.

The numerical experiences concerning elastic analysis permits showing that the cable stress increment, due to external loads, is usually smaller, besides being homogeneous, than the stress increment which occurs in the more classical case of cable continuously bounded to the beam, so that failure is usually related to stress concentration occurring in the beam. The distribution of relative slips between system components is also analysed showing the influence of the cable path and the kind of external action.

With reference to stability analysis, it was observed that the instabilizing effects related to the beam bending are balanced by the stabilizing contribution provided by the corresponding deformation of the stressed cable, for the geometries considered. On the other hand, the presence of the cable affects more strongly instabilizing phenomena related to torsional and shear deformations and their influence becomes more remarkable when torsional and shear deformability of the beam increases, as occurs in thin walled beams with open cross sections. However, such a phenomenon is strictly related to the geometry of the cable path and can furnish stabilising terms in some cases and instabilizing terms in other cases.

Some problems still open on the subject are finally recalled in the last section.

2. RECALLS ON THE PROBLEM FORMULATION

Here the balance conditions determined in (Dall'Asta & Leoni (1997)), and used for the following numerical analysis, are synthetically recalled referring to the previous work for notation and definitions of symbols involved.

Even if the work cited presented both variational and local formulation, in this paper only the former has been considered. The variational formulation generally has some advantages, with respect to the local formulation, which can also be evidenced in the problem in question. A first aspect deals with the major generality of the weak formulation which requires less regularity of the known and unknown functions in the equations. The second advantage is that the problem expressed in weak form can be numerically solved by means of the classical approximation methods of variational calculus.

In this specific problem the dependence of local balance on global beam deformation due to the slipping cable, translates into the integral-differential equations which constitute the local formulation of the problem and for which it is not possible to obtain a closed form solution. On the other hand, the presence of the slipping cable does not introduce further complications in the weak formulation with respect to classical elastic problems. However, in such a case the global structural coupling is reflected in the formal structure of terms related to the elastic deformation which is obtained by the product of two functionals linear in the admissible displacements while, in the case of bonded cables and generally in structures without relative slips, it would be constituted by a functional of a quadratic function. To conclude, the variational approach gives a more natural formulation of the physical problem and allows a straighter numerical solution.

The first balance condition of interest in the sequel is

$$\begin{aligned}
& \int_0^L \mathbf{K} \mathcal{D} \mathbf{v} \cdot \mathcal{D} \hat{\mathbf{v}} \, d\zeta + \frac{c}{\Lambda} \left(\int_0^L \boldsymbol{\Theta} \cdot \mathcal{D} \mathbf{v} \, d\zeta \right) \left(\int_0^L \boldsymbol{\Theta} \cdot \mathcal{D} \hat{\mathbf{v}} \, d\zeta \right) \\
& = -ce_0 \int_0^L \boldsymbol{\Theta} \cdot \mathcal{D} \hat{\mathbf{v}} \, d\zeta + \int_0^L \mathbf{q} \cdot \hat{\mathbf{v}} \, d\zeta + \mathbf{q}_\theta \cdot \hat{\mathbf{v}}_\theta |_{\theta=0,L} \quad \forall \hat{\mathbf{v}} \in C \quad (1)
\end{aligned}$$

which expresses the equilibrium of the system under external loads. The formulation describes the system behavior by starting from the reference configuration in which the beam is in its natural state (no stress) and furnishes adequate results in determining problem solutions for small strains and small displacements. The vector valued function \mathbf{v} represents the problem unknown and consists of the axis displacements components, cross section rigid rotations and warping functions, while \mathcal{D} is a differential operator furnishing generalized strains from displacements. The former term accounts for the beam elastic behavior and \mathbf{K} is related to the section stiffness while the second term accounts for the cable elastic behavior, c is the cable stiffness, Λ is the initial length, $\boldsymbol{\Theta}$ is a vector deriving from the cable path geometry. The first term on the right accounts for the cable stress ce_0 existing in the reference configuration while the last two terms are produced by external loads along the beam (\mathbf{q}) and at the basis (\mathbf{q}_θ). Finally, C is the space of kinematically admissible virtual displacements $\hat{\mathbf{v}}$.

The infinitesimal stability of balanced configurations are tested by means of the following condition

$$\begin{aligned}
\Psi(\mathbf{v}, \hat{\mathbf{v}}) &= \int_0^L \mathbf{K} \mathcal{D} \mathbf{v} \cdot \mathcal{D} \hat{\mathbf{v}} \, d\zeta + \frac{c}{\Lambda} \left(\int_0^L \boldsymbol{\Theta} \cdot \mathcal{D} \mathbf{v} \, d\zeta \right) \left(\int_0^L \boldsymbol{\Theta} \cdot \mathcal{D} \hat{\mathbf{v}} \, d\zeta \right) \\
&+ \tau_0^* \int_0^L (\mathbf{W}_\tau + \mathbf{W}^c) \mathcal{G} \mathbf{v} \cdot \mathcal{G} \hat{\mathbf{v}} \, d\zeta + \kappa \int_0^L [\tau_{0\kappa} (\mathbf{W}_\tau + \mathbf{W}^c) + \mathbf{W}_\kappa] \mathcal{G} \mathbf{v} \cdot \mathcal{G} \hat{\mathbf{v}} \, d\zeta > 0, \quad \forall \mathbf{v} = \hat{\mathbf{v}} \in C \quad (2)
\end{aligned}$$

obtained by linearizing the problem at a stressed balanced configuration and requiring the uniqueness of the solution for every small perturbation. The former two terms derive from the elastic stiffness of beam and cable and the latter two terms have a geometric nature and account for the stress existing in the beam and the force existing in the cable. They are decomposed by introducing a multiplier τ_0^* of the initial traction force induced in the cable and a multiplier κ of the external loads, so that the cable traction force consists of two contributes: τ_0^* and a term $\kappa\tau_{0\kappa}$ proportional to the applied loads. Differential operator \mathcal{G} provides the second order terms related to the displacement gradient while the algebraic operators \mathbf{W}^c , \mathbf{W}_τ and \mathbf{W}_κ , respectively, derive from the cable force contribution for unitary traction cable force, beam stress contribution for unitary cable traction force and beam stress contribution for unitary value of the load multiplier.

3. NUMERICAL SOLUTION

3.1. Solution approximation

In the following sections the classical Ritz (Courant and Hilbert (1953)) variational method will be utilised to obtain the numerical formulation of the elastic and the infinitesimal stability problems. Such a method is based on the assumption that the solution space of the problem \mathcal{U} is a Hilbert space. By considering a finite-dimensional subspace $\mathcal{U}_m \subset \mathcal{U}$, generated by the system $\{y_i\}$ ($i = 1, \dots, m$) constituted by the truncation of the first m terms of a complete function sequence in \mathcal{U} , each element $v \in \mathcal{U}$ can be approximated by the linear combination

$$\bar{v}(\zeta) = w_i y_i(\zeta). \quad (3)$$

The completeness of the sequences of subspaces implies that each $v \in \mathcal{U}$ can be approximated

by elements of subspaces U_m with every degree of precision in the sense of the norm of U . For the problem in question, in which the solution is a function $\mathbf{v}: \mathbb{R} \rightarrow \mathbb{R}^{10}$, the assumption is that U is given by the cartesian product of ten Hilbert spaces of functions satisfying kinematical boundary conditions; the i -th component of the unknown vector \mathbf{v} is thus approximated, by the first m_i terms of a complete function sequence, as

$$\bar{v}_i(\zeta) = w_{(i)j} y_{(i)j}(\zeta) \quad (j = 1 \dots m_i, \text{ no summation on } (i)) \quad (4)$$

which can be written in the vectorial form

$$\bar{v}_i(\zeta) = \mathbf{y}_{(i)}(\zeta) \cdot \mathbf{w}_{(i)}. \quad (5)$$

By recomposing the approximating vector $\bar{\mathbf{v}}(\zeta)$, from eqn (5) the expression

$$\bar{\mathbf{v}}(\zeta) = \mathbf{Y}(\zeta) \mathbf{w} = \begin{bmatrix} \mathbf{y}_{(1)}^T & \mathbf{0} & \cdots & \mathbf{0} \\ \mathbf{0} & \mathbf{y}_{(2)}^T & \cdots & \mathbf{0} \\ \vdots & \vdots & \ddots & \vdots \\ \mathbf{0} & \mathbf{0} & \cdots & \mathbf{y}_{(10)}^T \end{bmatrix}_{10 \times m} \begin{bmatrix} \mathbf{w}_{(1)} \\ \mathbf{w}_{(2)} \\ \vdots \\ \mathbf{w}_{(10)} \end{bmatrix}_{m \times 1} \quad (6)$$

is finally derived. Since matrix \mathbf{Y} collects the known functions of the abscissa ζ which constitutes the subspace base, vector \mathbf{w} , with $m = \sum_{i=1}^{10} m_i$ components, completely describes the approximated solution.

For the sake of simplicity, by considering the case of homogeneous principal boundary conditions, the space of the solution is linear and the admissible variations of the displacements $\hat{\mathbf{v}}$ can be approximated in the same way by

$$\hat{\mathbf{v}}(\zeta) = \mathbf{Y}(\zeta) \hat{\mathbf{w}}. \quad (7)$$

3.2. Elastic analysis

By substituting \mathbf{v} and the variations $\hat{\mathbf{v}}$, in the balance condition, with the approximations (6) and (7) one obtains a linear algebraic problem whose unknowns are the coefficients of the linear combination which fulfils the balance condition in the subspace $U_m \subset U$. The global balance condition (1) transforms into

$$\begin{aligned} & \int_0^L \mathbf{K} \tilde{\mathcal{D}} \mathbf{Y} \mathbf{w} \cdot \tilde{\mathcal{D}} \mathbf{Y} \hat{\mathbf{w}} \, d\zeta + \frac{c}{\Lambda} \left(\int_0^L \boldsymbol{\Theta} \cdot \tilde{\mathcal{D}} \mathbf{Y} \mathbf{w} \, d\zeta \right) \left(\int_0^L \boldsymbol{\Theta} \cdot \tilde{\mathcal{D}} \mathbf{Y} \hat{\mathbf{w}} \, d\zeta \right) \\ & + c e_0 \int_0^L \boldsymbol{\Theta} \cdot \tilde{\mathcal{D}} \mathbf{Y} \hat{\mathbf{w}} \, d\zeta - \int_0^L \mathbf{q} \cdot \mathbf{Y} \hat{\mathbf{w}} \, d\zeta - \mathbf{q}_g \cdot \mathbf{Y}_g \hat{\mathbf{w}}|_{g=0,L} = 0 \end{aligned} \quad \forall \hat{\mathbf{w}} \in \mathcal{R}^m \quad (8)$$

where operator $\tilde{\mathcal{D}}$, deriving from \mathcal{D} , maps matrices \mathbf{Y} into matrices with dimensions $14 \times m$

$$\tilde{\mathcal{D}} \mathbf{Y} = [\mathcal{D} \mathbf{Y}_1 \mathcal{D} \mathbf{Y}_2 \cdots \mathcal{D} \mathbf{Y}_m]_{14 \times m} \quad (9)$$

in which \mathbf{Y}_i ($i = 1, \dots, m$) are vectors whose components are the elements of the i -th column of matrix \mathbf{Y} . By considering that vectors \mathbf{w} and $\hat{\mathbf{w}}$ do not depend on the beam abscissa and can be extracted from integrals and by considering that condition (8) must hold for every $\hat{\mathbf{w}}$, it is possible to reduce the problem to the following linear system,

$$\mathbf{A} \mathbf{w} = \mathbf{l} \quad (10)$$

which is equivalent to condition (8) for invertible coefficient matrix \mathbf{A} having the expression

$$\mathbf{A} = \left[\int_0^L (\tilde{\mathcal{G}}\mathbf{Y})^T \mathbf{K} (\tilde{\mathcal{G}}\mathbf{Y}) d\zeta + \frac{c}{\Lambda} \left(\int_0^L (\tilde{\mathcal{G}}\mathbf{Y})^T \boldsymbol{\Theta} d\zeta \right) \otimes \left(\int_0^L (\tilde{\mathcal{G}}\mathbf{Y})^T \boldsymbol{\Theta} d\zeta \right) \right]_{m \times m}. \quad (11)$$

Under the assumption of stable elastic materials, \mathbf{A} is a symmetric and strictly positive definite matrix (commonly called Gramm matrix) describing the global stiffness of the cable-beam system. The vector which collects known terms of the problem, involving both external actions on the beam and pretension of the cable, has the following expression

$$\mathbf{l} = \left[-ce_0 \int_0^L (\mathcal{G}\mathbf{Y})^T \boldsymbol{\Theta} d\zeta + \int_0^L \mathbf{Y}^T \mathbf{q} d\zeta + \mathbf{Y}_g^T \mathbf{q}_g|_{g=0,L} \right]. \quad (12)$$

Since the dimensions of the problem are always not very large, inversion of matrix \mathbf{A} does not involve particular difficulties and can be performed by the Gauss–Jordan method. Once vector \mathbf{w} has been calculated from eqn (10), it is easy to obtain, by a back substitution, the approximated value of all the static and kinematical quantities defined in (Dall’Asta and Leoni (1997)); for example, the expressions of vector \mathbf{Q} of the active stress resultants (normal and shear forces, bending and twisting moments, bi-shear and bi-moments), the stress τ in the cable and the cable–tube relative slip δ , are reported in the sequel

$$\mathbf{Q}(\zeta) \cong \mathbf{K} \tilde{\mathcal{G}}\mathbf{Y}\mathbf{w}, \quad (13)$$

$$\tau \cong \frac{c}{\Lambda} \int_0^L \boldsymbol{\Theta} \cdot \tilde{\mathcal{G}}\mathbf{Y}\mathbf{w} d\zeta + ce_0, \quad (14)$$

$$\delta(\zeta) \cong \int_0^L (\tilde{\mathcal{G}}\mathbf{Y})^T \boldsymbol{\Theta} \cdot \mathbf{w} d\zeta - \left(1 + \frac{1}{\Lambda} \int_0^L \boldsymbol{\Theta} \cdot \tilde{\mathcal{G}}\mathbf{Y}\mathbf{w} d\zeta \right) \Lambda(\zeta). \quad (15)$$

where $\Lambda(\zeta)$ denotes the initial length of the cable path from the first anchorage up to the abscissa ζ .

3.3. Infinitesimal stability

An approximated test of the cable-beam system infinitesimal stability can always be obtained in the subspace of the admissible displacements U_m spanned by the Ritz basis functions according to eqn (6). By substituting the approximated value $\hat{\mathbf{v}}$ into the stability condition (2) the following discrete condition can be obtained

$$\begin{aligned} \Psi = & \left(\int_0^L (\tilde{\mathcal{G}}\mathbf{Y})^T \mathbf{K} (\tilde{\mathcal{G}}\mathbf{Y}) d\zeta \right) \mathbf{w} \cdot \hat{\mathbf{w}} \\ & + \left[\frac{c}{\Lambda} \left(\int_0^L \boldsymbol{\Theta} \cdot (\tilde{\mathcal{G}}\mathbf{Y}) d\zeta \right) \otimes \left(\int_0^L (\tilde{\mathcal{G}}\mathbf{Y})^T \boldsymbol{\Theta} d\zeta \right) \right] \mathbf{w} \cdot \hat{\mathbf{w}} \\ & + \tau_0^* \left(\int_0^L (\tilde{\mathcal{G}}\mathbf{Y})^T (\mathbf{W}_\tau + \mathbf{W}^c) (\tilde{\mathcal{G}}\mathbf{Y}) d\zeta \right) \mathbf{w} \cdot \hat{\mathbf{w}} \\ & + \kappa \left(\int_0^L (\tilde{\mathcal{G}}\mathbf{Y})^T [\tau_\lambda (\mathbf{W}_\tau + \mathbf{W}^c) + \mathbf{W}_\kappa] (\tilde{\mathcal{G}}\mathbf{Y}) d\zeta \right) \mathbf{w} \cdot \hat{\mathbf{w}} > 0 \quad \forall \mathbf{w} = \hat{\mathbf{w}} \in \mathbb{R}^m \end{aligned} \quad (16)$$

where operator $\tilde{\mathcal{G}}$ derives from \mathcal{G} and is defined by

$$\tilde{\mathcal{G}}\mathbf{Y} = [\mathcal{G}\mathbf{Y}_1 \mathcal{G}\mathbf{Y}_2 \cdots \mathcal{G}\mathbf{Y}_m]_{14 \times m} \quad (17)$$

in which, once again, \mathbf{Y}_i ($i = 1, \dots, m$) are vectors whose components are the elements of

the i -th column of matrix \mathbf{Y} and $\tilde{\mathcal{Y}}$ consists of a matrix with the dimensions $14 \times m$. By recalling the definition (11) of matrix \mathbf{A} and defining the further symmetric matrices

$$\mathbf{B}^\tau = \left[\int_0^L (\tilde{\mathcal{Y}}^\top)^T (\mathbf{W}_\tau + \mathbf{W}^c) (\tilde{\mathcal{Y}}) d\zeta \right]_{m \times m}, \quad (18)$$

$$\mathbf{B}^\kappa = \left[\int_0^L (\tilde{\mathcal{Y}}^\top)^T [\tau_\kappa (\mathbf{W}_\tau + \mathbf{W}^c) + \mathbf{W}_\kappa] (\tilde{\mathcal{Y}}) d\zeta \right]_{m \times m}, \quad (19)$$

condition (16) can be rewritten in vectorial form as

$$\Psi = (\mathbf{A} + \tau_0^* \mathbf{B}^\tau + \kappa \mathbf{B}^\kappa) \mathbf{w} \cdot \hat{\mathbf{w}} > 0 \quad \forall \mathbf{w} = \hat{\mathbf{w}} \in \mathbb{R}^m. \quad (20)$$

The previous relation is the condition ensuring that matrix $\mathbf{A} + \tau_0^* \mathbf{B}^\tau + \kappa \mathbf{B}^\kappa$ is strictly positive definite. By analysing each term of (20) information on the system can be obtained. Under the assumption of stable material for the considered stress, the first matrix is strictly positive definite, similarly to that observed in (Dall'Asta and Leoni (1997)) for the corresponding continuous operator. On the other hand, the remaining two terms may be indefinite and so may generate instability of the system. At this point all the problems connected with the stability of the structure can be numerically solved, namely the stabilising or instabilising role of the cable path can be recognized, the critical cable stress can be calculated and the interaction between cable stress and critical external loads can be evaluated.

The first problem is simple to solve by observing that the numerical form of the condition ensuring the stabilizing role of the cable path (corresponding to condition (70) of Dall'Asta and Leoni (1997)), is

$$\mathbf{B}^\tau \hat{\mathbf{w}} \cdot \hat{\mathbf{w}} > 0 \quad \forall \hat{\mathbf{w}} \in \mathbb{R}^m. \quad (21)$$

Since \mathbf{B}^τ is a real and symmetric matrix, condition (21) holds if and only if all eigenvalues of \mathbf{B}^τ are strictly positive. This means that a simple test to recognise stabilizing paths consists in evaluating the minimum eigenvalue of \mathbf{B}^τ and testing if it is major than zero. Since matrix \mathbf{B}^τ is symmetric and has small dimensions the Jacobi procedure can be adopted to extract its eigenvalues (Bathe and Wilson, (1976)).

The second problem, namely to calculate the critical cable stress when the cable path is instabilising, can be numerically solved by setting $\kappa = 0$ and seeking for \mathbf{w} such that $\Psi(\mathbf{w}, \mathbf{w}) = 0$. This originates the eigenvalue problem

$$(\mathbf{A} + \tau_0^* \mathbf{B}^\tau) \mathbf{w} = 0 \quad (22)$$

which, by using the Cholesky factorization $\mathbf{B}^\tau = \tilde{\mathbf{B}}^\tau (\tilde{\mathbf{B}}^\tau)^\top$ and by defining $\tilde{\mathbf{w}} = \tilde{\mathbf{B}}^\tau \mathbf{w}$ and $\tilde{\mathbf{A}} = (\tilde{\mathbf{B}}^\tau)^{-1} \mathbf{A} (\tilde{\mathbf{B}}^\tau)^{-\top}$, can be reduced to the standard form

$$(\tilde{\mathbf{A}} + \tau_0^* \mathbf{I}) \tilde{\mathbf{w}} = 0. \quad (23)$$

Once again, the Jacobi procedure can be adopted by extracting eigenvalues of the symmetric matrix $\tilde{\mathbf{A}}$. The minimum eigenvalue τ_0^* of problem (23) represents an upper bound approximation of the critical cable stress τ_{0cr}^* when the beam is subjected to prestressing only, while the corresponding eigenvector permits obtaining an approximation of the first instabilising mode by means of the following transformation

$$\mathbf{v} = \mathbf{Y} (\tilde{\mathbf{B}}^\tau)^{-1} \tilde{\mathbf{w}}. \quad (24)$$

Finally, the third problem to determine the critical multiplier of the external loads for

a fixed value of the initial cable stress τ_0^* can be obtained by imposing the critical condition $\Psi = 0$. This translates into a further eigenvalues problem

$$[(\mathbf{A} + \tau_0^* \mathbf{B}^T) + \kappa \mathbf{B}^K] \mathbf{w} = 0 \tag{25}$$

which, exactly as in the previous case, can be reduced to the standard form

$$(\tilde{\mathbf{A}} + \kappa \mathbf{I}) \tilde{\mathbf{w}} = 0. \tag{26}$$

where, $\tilde{\mathbf{B}}$ is the Cholesky factor of matrix \mathbf{B}^K , $\tilde{\mathbf{w}} = \tilde{\mathbf{B}}^K \mathbf{w}$ and $\tilde{\mathbf{A}} = (\tilde{\mathbf{B}}^K)^{-1} (\mathbf{A} + \tau_0^* \mathbf{B}^T) (\tilde{\mathbf{B}}^K)^{-T}$. An upper bound estimation of the multiplier κ_{cr} is represented by the minimum eigenvalue of problem (26) which can be calculated by the Jacobi procedure. Similarly to the previous case, the corresponding eigenvector permits approximating the first instabilising mode of the beam by the relation

$$\mathbf{v} = \mathbf{Y}(\tilde{\mathbf{B}}^K)^{-1} \tilde{\mathbf{w}}. \tag{27}$$

4. WORK EXAMPLES

Prestressing by slipping cables of thin walled beams with open cross section (often realized in steel or concrete) has an important use in the construction of bridges or civil structure decks. Usually, prestressing of such beams is carried out before subsequent assembly with other structural elements so that, during the first building stages (e.g., when upper slabs or lateral stiffeners have not yet been realised), the prestressed beam is restrained only at the end cross sections. During such phases flexural-torsional buckling may occur due to the low torsional stiffness of the beam cross section. It should be noted that with regard to steel beams, for which internal prestressing cannot be carried out, the case studied has to be reviewed as a limit case in which the cable path is fixed by a great number of deviation devices. The coupling model previously proposed is applied to some cases of thin walled beams prestressed both by curved and straight cables paying attention to the linear elastic behavior of the cable-beam system and to the instability phenomena previously mentioned.

Two kinds of "I" cross sections (Table 1), are considered. They are characterised by different wall thicknesses, related to the cross section dept H, in order to study the behaviour of typical steel and concrete cross sections. A simply supported beam is considered, longitudinal translations are prevented at one end, twisting rotation is obstructed at both the ends while any warping can occur. Prestressing is carried out by means of internal straight or parabolic cables lying on the symmetric plane of the cross section and respectively following the two paths

Table 1. Cross sections and static scheme of work examples

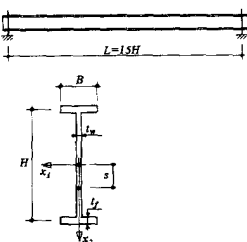
		Steel beam	Concrete beam
	$G = 0.4E$	$B = \frac{H}{5}$	$B = \frac{H}{5}$
	$c = 0.1EA$	$t_w = \frac{1}{100}H$	$t_w = \frac{1}{20}H$
		$t_f = 2t_w = \frac{1}{50}H$	$t_f = 1.5t_w = \frac{1.5}{20}H$

Table 2. Ritz function sequences adopted

u_1, u_2, φ_3	$f_i(\zeta) = \sqrt{\frac{2}{L}} \sin\left(\frac{i\pi\zeta}{L}\right) \quad i = 1, 2, \dots$
u_3	$f_1(\zeta) = \frac{\zeta}{L} \sqrt{\frac{3}{L}}$
	$f_i(\zeta) = \sqrt{\frac{2}{L}} \sin\left[\frac{(i-1)\pi\zeta}{L}\right] \quad i = 2, \dots$
φ_1, φ_2	$f_1 = 1$
$\chi_0, \chi_1, \chi_2, \chi_3$	$f_2 = \zeta$
	$f_i = 2f_{i-1}\zeta - f_{i-2} \quad i = 3, 4, \dots$

$$\mathbf{H}(\zeta) = s\mathbf{A}_2 + \zeta\mathbf{A}_3, \quad (28)$$

$$\mathbf{H}(\zeta) = \left\{ (2H - 4s) \left[\left(\frac{\zeta}{L}\right) - \left(\frac{\zeta}{L}\right)^2 + s \right] \right\} \mathbf{A}_2 + \zeta\mathbf{A}_3, \quad (29)$$

in which s is the cable anchorage x_2 -ordinate at the end cross sections, \mathbf{A}_3 is the unit vector lying along the beam axis, \mathbf{A}_1 and \mathbf{A}_2 are the unit orthogonal vectors to which x_1 and x_2 are referred (see Table 1). The two classical load conditions constituted by uniformly distributed load applied at the upper flange of the beam and by two bending moments applied at the end cross sections of the beam, are considered.

The importance of shear strain, which generally occurs on the mean wall surface of the beam, suggests the use of a model which is able to describe with sufficient precision the loss of planarity of the cross sections. The model proposed in (Laudiero and Savoia, 1991) which adopts ten kinematic descriptors depending on the beam abscissa ζ only, is adopted. In addition to the six parameters describing the cross section rigid motions, warping displacements due to primary and non uniform torsion, as well as to shear forces, are taken into account. The normalised warping functions adopted in the analysis are calculated as in (Laudiero and Savoia, 1991).

The numerical solution of the problem is performed according to the Ritz approximation method by assuming truncation of a normalised sinusoidal sequence as shape functions for translations u_1 , translations u_2 and twisting rotations of cross sections φ_3 , while truncations of the Tschebichef polynomial sequence are adopted for the other descriptors (bending rotations φ_1 and φ_2 and warping intensities χ_0, χ_1, χ_2 and χ_3). With regard to the axial translation of the cross section described by u_3 , a linear function is joined to a sinusoidal expansion in order to fulfil the boundary conditions (see Table 2).

Even if the model can describe very complex displacements fields, geometry of the working example and the kinds of external actions considered allow an *a priori* reduction of the solution space in the case of elastic analysis by setting $u_1 = \varphi_2 = \varphi_3 = \chi_0 = \chi_1 = \chi_3 = 0$. On the other hand it is well known that, in the case of stability analysis, the solution space cannot be reduced; however it is interesting to observe that geometry of the cross section of the work examples, which show very different stiffness with respect to the two principal directions, suggest favoring just the displacement functions which were identically null in the elastic analysis (tests on the solution convergence confirmed this fact).

5. ELASTIC ANALYSIS

This section reports some results of the elastic analysis obtained from condition (8). The two different kinds of beam in which prestressing is carried out with cables following the parabolic path (29) are considered. The numerical applications described show the relations existing between cable stress progress and cable geometry, providing a comparison

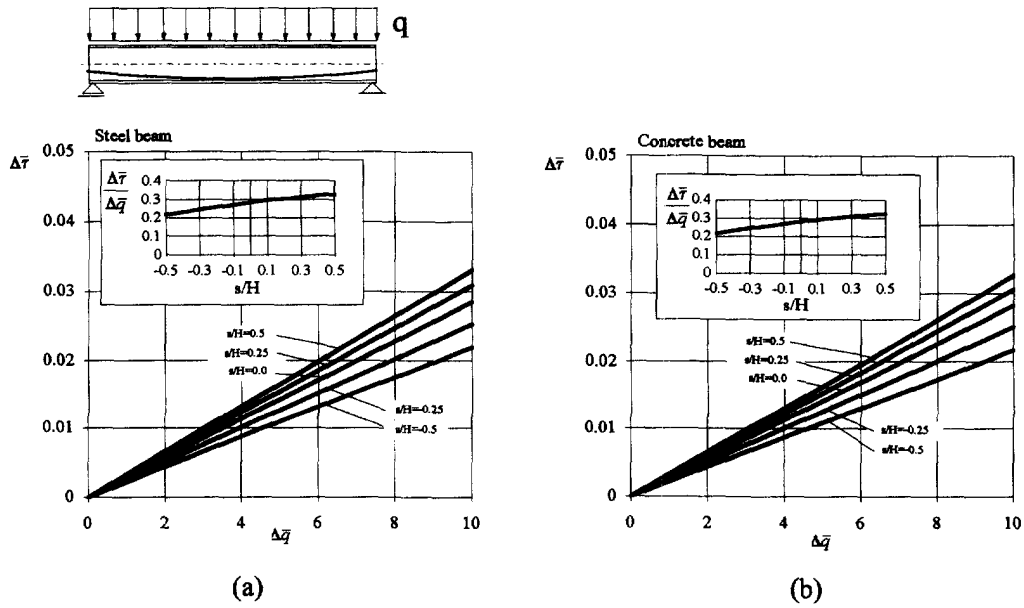


Fig. 1. Cable stress increment versus external distributed local increment: (a) steel beam; (b) concrete beam.

between such a system and the alternative system where the cable is continuously bonded to the beam and evaluating the relative slip occurring between cable and beam.

In Fig. 1, the non dimensional value of the cable stress increment ($\Delta\bar{\tau} = \Delta\tau/EA \times 1000$) versus the non dimensional increment of the external loads ($\Delta\bar{q} = \Delta qL^2H/EI_1 \times 1000$) are plotted. In order to show the influence of the cable path on the increment of the cable stress, analysis is repeated by varying the non dimensional parameter s/H —which describes the cable eccentricity at the end cross sections of the beam—between the value $s/H = 0.5$ (straight cable running along the bottom flange of the beam) and $s/H = -0.5$ (parabolic cable with maximum curvature). Obviously, the curves reported are straight lines since a linear elastic analysis was performed. The slope of such straight lines strongly varies with the cable geometry, decreasing from the straight path ($s/H = 0.5$) to the curved ones. Furthermore, the diagram of the straight line slopes versus eccentricity of the cable anchorage shows a slightly major sensitiveness to the changing of the path for the cable anchored at the lower part of the beam (almost straight cables) than those anchored at the upper part (high curved cables). It is important to underline that such increments are not very important, since they result in only a small fraction of the controlled prestressing. The comparison between the steel and concrete beams shows a substantial equivalence of their behavior; in fact the diagrams, reported just for the sake of completeness, are almost identical. Quite similar results are shown in Fig. 2 where the increments of the cable stress due to the increment of the bending moments applied at the beam ends are reported (the diagram reports the non dimensional $\Delta\bar{M} = \Delta MH/EI_1 \times 1000$). In this case the slope of the curves is higher than in the previous case.

Figs 3 and 4 show the substantial difference which exists between the behavior of bonded and unbonded cables. As already observed in Dall'Asta and Leoni (1997), in the case of unbonded cables, the global coupling between cable and beam translates into the mathematical model structure. In fact, the global balance condition is characterized by the term related to the cable stress obtained as product of two terms of global deformation (eqn (8)). On the contrary, in the case of bonded cables, the system Gramm matrix assumes the form

$$A = \left[\int_0^L \left\{ (\tilde{\mathcal{Y}})^T \mathbf{K} (\tilde{\mathcal{Y}}) + \frac{c}{|\mathbf{H}'|} [(\tilde{\mathcal{Y}})^T \boldsymbol{\Theta}] \otimes [(\tilde{\mathcal{Y}})^T \boldsymbol{\Theta}] \right\} d\zeta \right]_{m \times m} \quad (30)$$

in which the term related to the cable, similarly to the beam term, is constituted by the

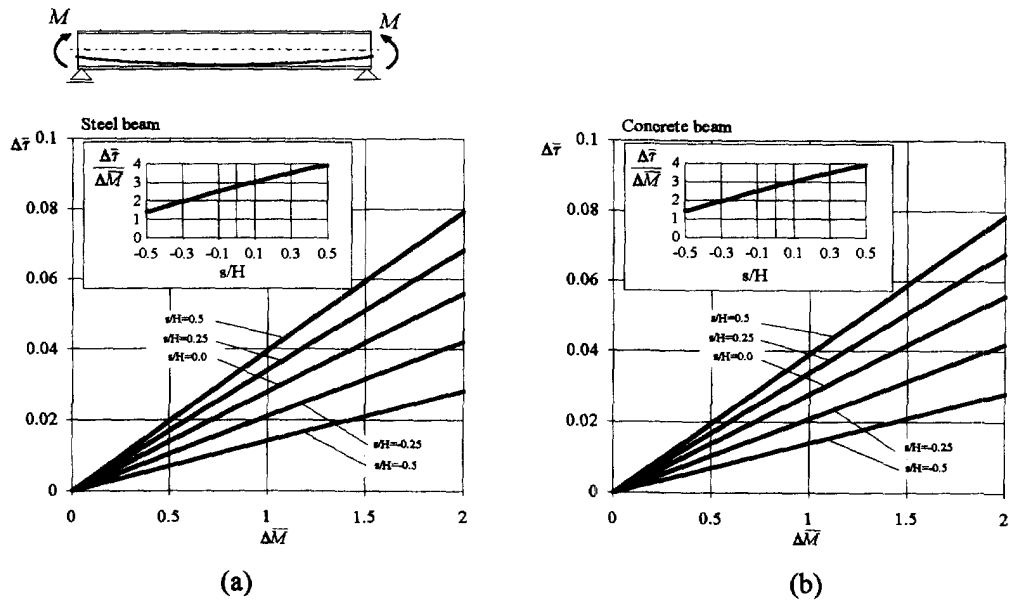


Fig. 2. Cable stress increment versus end bending moment increment : (a) steel beam ; (b) concrete beam.

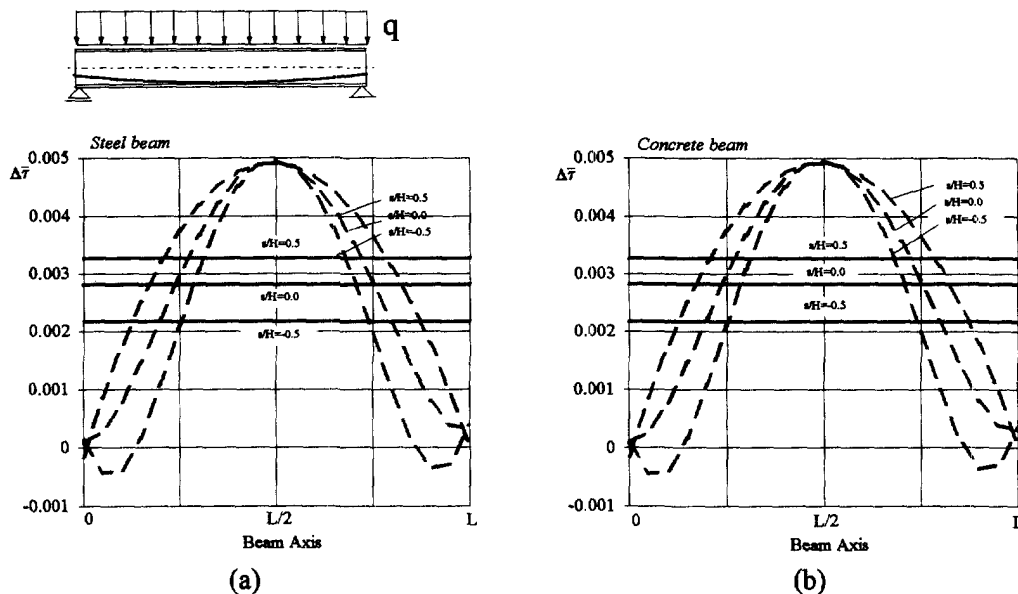


Fig. 3. Comparison between bonded and unbonded prestressing cable — cable stress increment due to a unitary increment of the non dimensional distributed load : (a) steel beam ; (b) concrete beam.

integral of the quadratic form obtained by the product of two terms of local deformation. This is reflected by a relative small major stiffness of the structure and, more so, by the fact that the cable stress variation are obviously variable along its path. Under the same increment of external load, the uniform variation of the stress in the slipping cable is about equal to the average stress increment in the bonded cable (Figs 3, 4) and, only in very particular cases such as those in which the bonded cable undergoes uniform stretch along its path (e.g., straight cable and external actions constituted by end bending moments (Fig. 4)), equivalent stress increments exist.

Diagrams of the cable-tube slip are reported in Figs 5 and 6. Since the load is symmetric, all the curves equal zero value at midspan. Slips are higher in the case of curved cables while they tend sensibly to reduce in the case of about straight cables. Obviously, slip distribution and sensibility to the cable path depend on the type of external action. It is, in

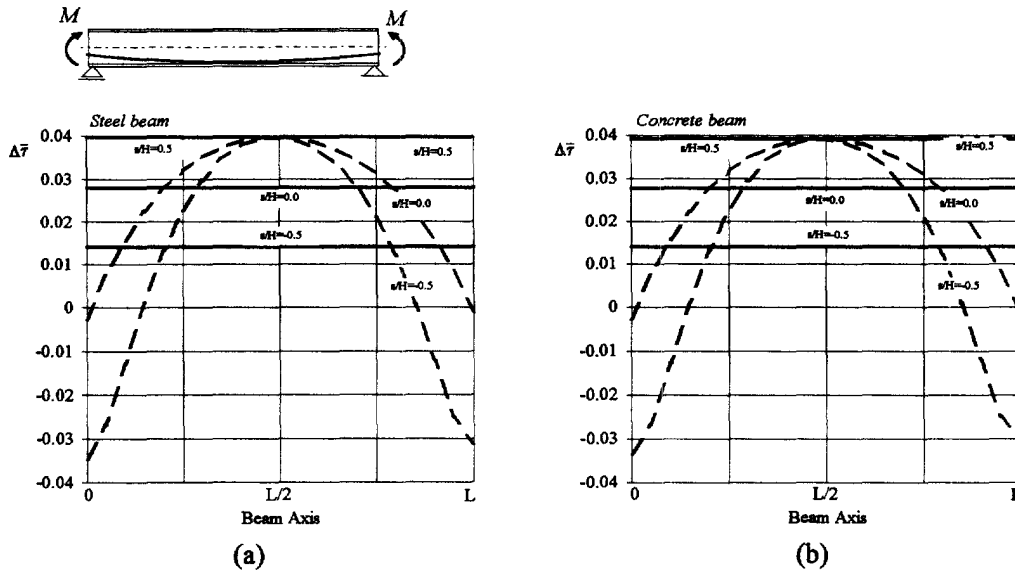


Fig. 4. Comparison between bonded and unbonded prestressing cable — cable stress increment due to a unitary increment of the non dimensional moment : (a) steel beam ; (b) concrete beam.

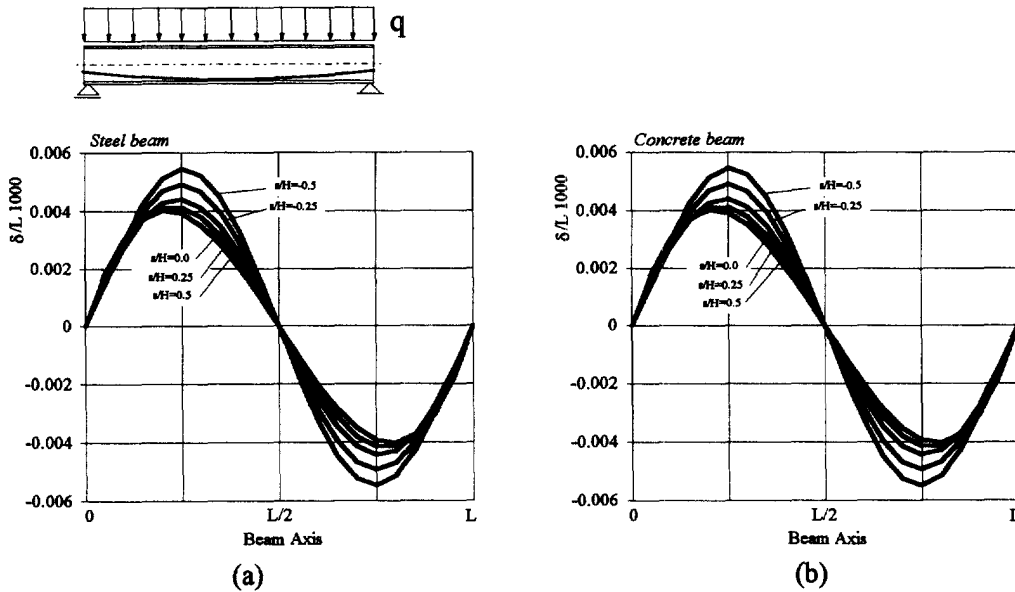


Fig. 5. Cable-tube slip due to a unitary increment of the non dimensional distributed load : (a) steel beam ; (b) concrete beam.

fact, notable that when the external action is constituted by end bending moments a particular case (straight cable $s/H = 0.5$), in which slips are zero, exists. This is because the constant bending moment along the beam induces constant local deformations of the longitudinal fibres so that the local deformation of the slipping cable is the same as that of the beam fibres. This relates to the previous statements involving comparison of the slipping and bonded cable behaviors.

The straight cables following path (28) are not considered in the elastic analysis since they provide no further information.

6. STABILITY ANALYSIS

This section analyses the stability of the system showing the interaction between prestressing and external loads. Figures 7 and 8 show the results obtained for the two kinds

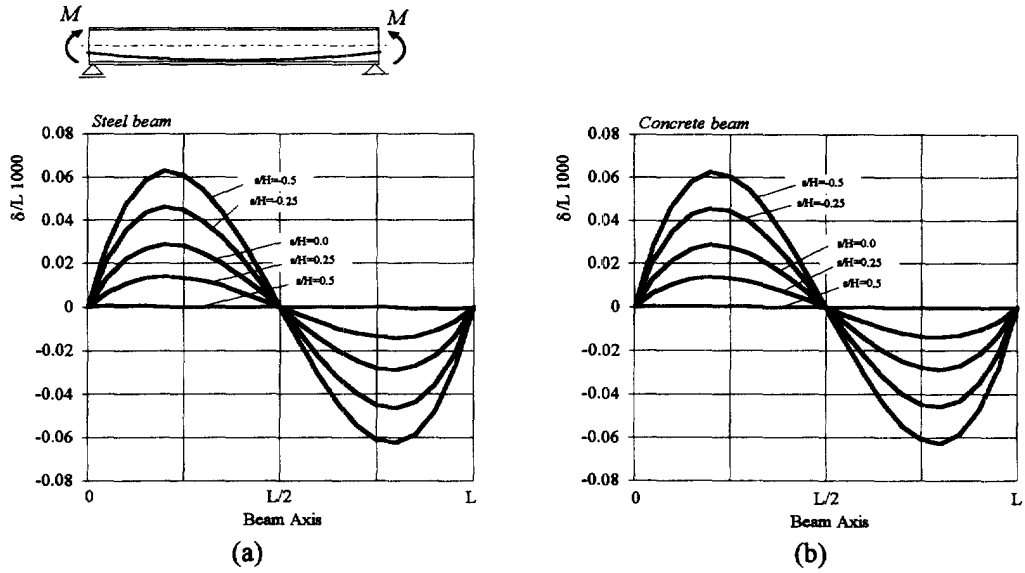


Fig. 6. Cable-tube slip due to a unitary increment of the non dimensional moment : (a) steel beam ; (b) concrete beam.

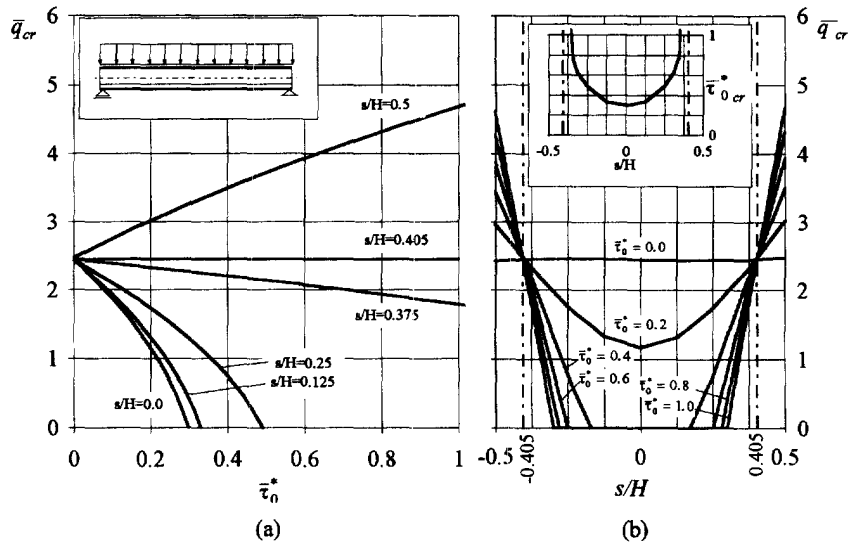


Fig. 7. Steel beam-straight cable : (a) critical load vs initial cable stress ; (b) critical load vs cable position.

of cross sections previously defined when prestressing is carried out with straight internal cables placed along the path (28). In particular, the influence of the initial cable stress τ_0^* (diagrams report the non dimensional quantity $\bar{\tau}_0^* = \tau_0^*/EA \times 1000$), which leads to flexural-torsional buckling, is evidenced in Figs 7a and 8a. Curves obtained for different values of s , branch out approximately from the same point corresponding to the zero initial stress for the cable. In this case q_{cr} is almost equal to that obtained analysing the problem without the cable. Figures 7b and 8b show the same result, from another point of view, plotting q_{cr} versus the cable position s for fixed stress τ_0^* . In fact it is immediately evident that the curve relevant to $\tau_0^* = 0$ is quite close to being a straight line. This makes it possible to conclude that the cable elastic stabilising term, and those related to the stress increment τ_{0k} induced by the external loads, are not very important in terms of evaluating the external critical load.

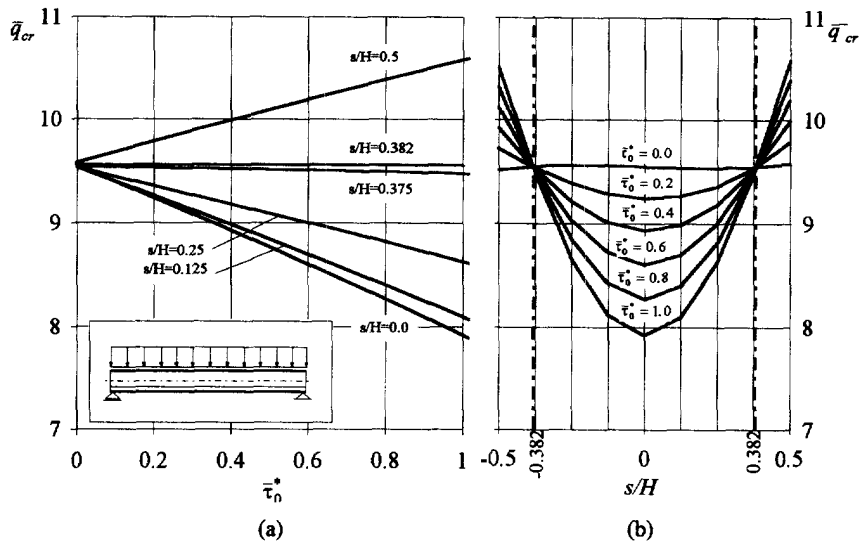


Fig. 8. Concrete beam-straight cable: (a) critical load vs initial cable stress; (b) critical load vs cable position.

Prestressing influence on the system equilibrium quality becomes evident by increasing τ_0^* . Curves $q_{cr} - \tau_0^*$ with positive slope (Figs 7a and 8a) are related to a cable characterised by a stabilising path, while curves characterised by negative slope are related to a cable lying on an instabilising path. Obviously, a path exists for which the cable initial stress τ_0^* does not influence the critical values of the external load. For such a path, curves $q_{cr} - \tau_0^*$ are horizontal straight lines (Figs 7a and 8a). This is also reflected on the diagrams of Figs 7b and 8b in which the two intersection points of curves related to different τ_0^* are evident. In the examined case of straight cables, two indifferent paths, approximately symmetric with respect to the beam axis, exist. With a simpler Vlasov model, Dall'Asta (1995) evidenced that the indifferent path is placed, with good approximation, at a distance from the cross section centroid about equal to the polar radius $\rho_p = \sqrt{(I_1 + I_2)/A}$. In the case of instabilising path, a cable stress τ_{0cr}^* , for which the equilibrium configuration is infinitesimally instable even in absence of external loads, always exists. Even if such values are usually very high for concrete beams to be incompatible with both the hypothesis of infinitesimal deformations and the material strength (Fig. 8a), they may be in the range of practical interest for steel beams (Fig. 7a). For this later case, critical values of the cable stress versus the cable position are plotted in the diagram internal to Fig. 7b. Vertical asymptotes are placed in correspondence of the indifference cable path positions. In the case of the concrete beam, even if the results are not as evident as those obtained for the steel beam, appreciable variations (from -20% up to $+15\%$) in the external critical load, with respect to those obtainable without prestressing, occur. It can also be observed that the system is very sensitive to the variation of the cable position for the paths placed in the more eccentric zones of the cross sections (Figs 7b and 8b). It is notable that the results shown are in agreement with those stated in (Magnel (1956)) for a beam prestressed by a centroid straight slipping cable in that the instabilising mode induced by prestressing in the case $s/H = 0.00$ is exclusively torsional and not of the Euler (flexural buckling) or Prandtl (flexural-torsional buckling) kinds.

Figures 9–12 show the results obtained with the parabolic cable path (29). The numerical tests were carried out by considering the distributed load at the upper flange of the beam (Figs 9 and 10) and the bending moments at the ends of the beam (Figs 11 and 12).

The results can be interpreted exactly in the same manner as those obtained with straight prestressing cables. It is in fact possible to note that the cable path may have a stabilising or instabilising influence on the system equilibrium quality. The particularity of the problem characterised by curved cables is that, in addition to longitudinal normal stresses, interaction with the cable induces important shear stress (t_{3z}) and transversal

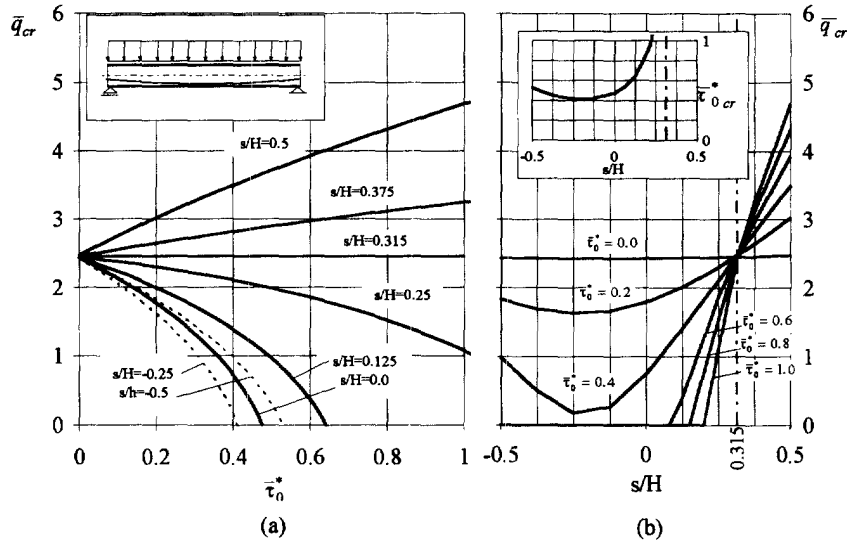


Fig. 9. Steel beam-curved cable: (a) critical load vs initial cable stress; (b) critical load vs cable position.

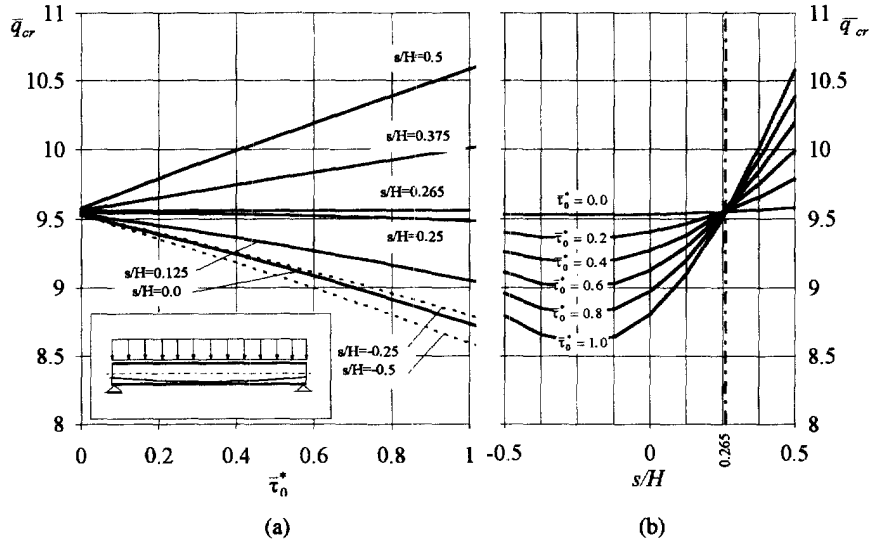


Fig. 10. Concrete beam-curved cable: (a) critical load vs initial cable stress; (b) critical load vs cable position.

normal stress (t_{ss}) on the wall of the beam. Depending on the crossing point of the prestressing cable with respect to the shear center, such stresses may generate stabilising or instabilising geometrical effects; in particular the latter generally increase with the eccentricity of the cable while the geometrical effects due to the longitudinal stress induced by prestressing tend to become instabilising (see the case of straight cables). Furthermore the secondary effects of the stretched cable have to be considered, these are always stabilising and as large as the eccentricity of the cable itself. Generally it is very difficult to predict the way in which each term due to prestressing influences the stability of the system so that an accurate analysis, involving all the various terms, must be performed.

Diagrams obtained in the case of distributed load on the upper flange of the beam are similar to those previously seen and show only a slightly lower sensitivity of the system to prestressing. In fact, stabilising paths are characterised by higher values of the critical stresses $\bar{\tau}_{0cr}^*$ with respect to those obtained with straight cables. Furthermore, curves of Figs 9a and 9b show that the path for which no influence on the external critical load exists is unique. Finally it should be noted that the cable-beam system is very sensitive to the

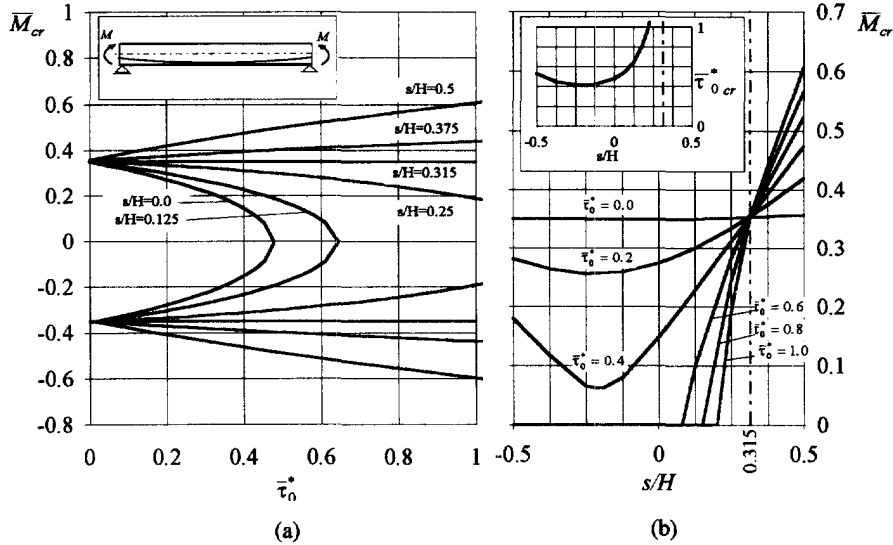


Fig. 11. Steel beam-curved cable : (a) critical moment vs initial cable stress ; (b) critical moment vs cable position.

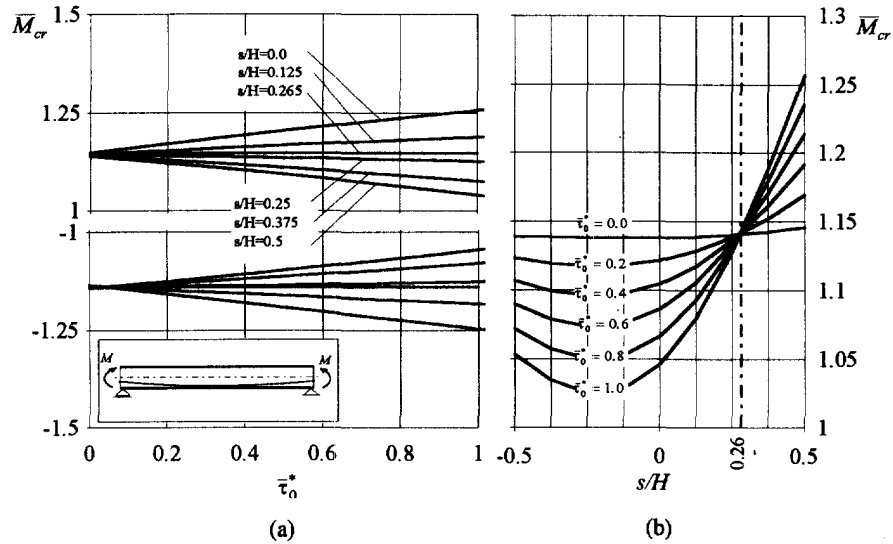


Fig. 12. Concrete beam-curved cable : (a) critical moment vs initial cable stress ; (b) critical moment vs cable position.

variation of the anchorage position for the eccentric zones in the lower part of the cross section, while by varying the anchorage position in the upper part of the cross section, lower variations in the critical external load are obtained, as also shown by the dashed curves plotted in Figs 4a and 5a related to paths with anchorages in the upper part of the cross section.

When the external action is constituted by two bending moments at the ends of the beam, the results are very similar to those obtained with distributed load. In this case the negative branches of curves $\bar{M}_{cr} - \bar{\tau}_0^*$ are also reported in Figs 11a and 12a (diagrams report the non dimensional quantity $\bar{M}_{cr} = M_{cr}H/EI_1 \times 1000$). They are almost symmetric to the positive branches with respect to the abscissa axis. This is due to the fact that the ending moments do not produce wall normal stresses with instabilising geometrical effects. With the same cable paths, for the initial stresses $\bar{\tau}_0^*$ close to the eventual $\bar{\tau}_{0,cr}^*$, bending moment critical values reduce more quickly than those of distributed load which, on the other hand, approach the zero value corresponding to $\bar{\tau}_{0,cr}^*$ more gradually.

7. CONCLUSIONS AND OPEN PROBLEMS

The problem of determining balanced configuration and testing their infinitesimal stability was numerically solved by starting from previously stated balance conditions in variational form.

Applications considering thin walled beams prestressed by straight or parabolic cables were developed. The considered geometries and external action levels permit applying the results to concrete and steel beams. Attention was focused on the influence of the cable prestressing force and cable path on the global stiffness, stress distribution under external loads and critical conditions by evidencing some aspects which are otherwise difficult to foresee without an appropriate coupling model.

The main characteristic aspect observed in the elastic behavior of such a system under external loads consists in the small increments of cable force. This is due to the frictionless contact and permits adopting large prestressing forces to the cable. The results were compared with those obtained for the classical case of cable rigidly connected to the beam.

With reference to the stability analysis, in the case of steel beams it was shown that the critical values of the cable stretching force, which can lead to infinitesimal instability even without external loads, exist in the range of practical applications. The cable force induces mainly torsional instability while it is possible to apply large cable force without risk of bending instability, so that the problem can practically be solved by introducing a sufficient number of lateral stiffeners.

Even if usual geometries makes concrete beams less sensitive to instability induced by prestressing, appreciable variations on the external critical load level occur and must be taken into account in design.

In the analyzed cases, the stabilizing or instabilizing effect of the cable is principally imputable to geometrical effects related to the beam and cable, while the contribution due to the elastic behavior of the cable is negligible and the structural elastic stiffness is mainly provided by the beam.

However, many other problems concerning the behavior of beams coupled, without friction, with stretched cables must yet be investigated in the range of the deformation linear theory. Insufficient information exists on the consequences of cables draped along a three-dimensional path or a plane path lying out of the principal bending planes. Furthermore, a deeper investigation of the interaction arising on curved beams is of interest in structural engineering.

The considerations presented in this paper descend from a kinematical model with transversally rigid section and only permitted evaluating global stability while it is probably of interest to develop an analysis based on a more refined kinematical model also able to evidence local instability phenomena.

Often beam and cable are not coupled along a regular curve but only at a finite number of saddle points. In this case the sensitiveness to instability is larger, as proved in (Dall'Asta (1996)), and deeper investigation is needed.

Recent applications in structural engineering were carried out by using innovative materials as FRP (Fiber Reinforced Plastic). In this case, the ratio between material strength and stiffness can be higher than the ratios used in the applications reported, referring to concrete and steel, and the stability analysis becomes more significant (Kelly (1989)).

Other aspects of interest concern the possibility of producing finite and controlled displacements in deformable rods. However, such a problem cannot be approached in the framework presented based on the infinitesimal deformation theory but involve fully nonlinear kinematical models, as adopted in (Dall'Asta and Leoni (1995)), or other intermediate models, considering small strains and large displacements (Wempner (1981)).

REFERENCES

- Bathe, K. J. and Wilson, E. L. (1976) Numerical methods in finite element analysis. Prentice-Hall, Inc.
 Courant, R. and Hilbert, D. (1953) *Methods of Mathematical Physics*. Vol. II. Interscience, New York.
 Dall'Asta, A. (1996) On the coupling between three dimensional bodies and slipping cables. *International Journal of Solids and Structures* 33(24), 3587-3600.

- Dall'Asta, A. and Leoni, G. (1997) Thin walled beams with internal unbonded cables: balance conditions and stability. *International Journal of Solids and Structures* (accepted).
- Dall'Asta, A. and Leoni, G. (1995) Alcune considerazioni sui solidi prismatici con cavi interni scorrevoli. In *Proceedings of AIMETA '95*, Napoli 3-6 October 1995, Vol. Meccanica delle Strutture I, pp. 345-350 (in Italian).
- Laudiero, F. and Savoia, M. (1990) Shear strain effects in flexure and torsion of thin-walled beams with open or closed cross-section. *Thin Walled Structures* **10**, 87-119.
- Magnel, X. (1956) *Theorie und Praxis des Spannbetons*. Wiesbaden, Berlin.
- Kelly, A. (1989) *Concise Encyclopedia of Composite Materials*. Pergamon Press, Oxford.
- Wempner, G. (1981) *Mechanics of Solids with Applications to Thin Bodies*. Sijthoff & Noordhoff, LOCATION, pp. 17-71.